Measurement of Magnitude and Phase of Harmonics Generated in Nonlinear Microwave Two-Ports

URS LOTT, STUDENT MEMBER, IEEE

Abstract—A new method for simultaneously measuring the magnitude and phase of the harmonics generated by a microwave two-port is reported. The two-port under test is driven with a sinusoidal microwave signal strong enough to force it into nonlinear operation. Its output harmonics are measured in the frequency domain with a setup which includes a vector network analyzer. For phase calibration at the harmonic frequencies, a millimeter-wave Schottky diode is used as a reference device.

Measurement results for the first four harmonics generated in a commercial GaAs MESFET under large-signal operation are presented. To show the validity of the phase measurement, the time-domain waveform constructed from the frequency-domain measurement data is compared to a direct time-domain measurement of the same device with a sampling oscilloscope.

I. Introduction

MODERN measurement systems for microwave devices should produce data suitable for fitting (equivalent circuit) device models—or at least for verification of existing models. In the linear operating range, microwave S-parameter measurements fill this need [1]. In contrast, the models used in nonlinear computer simulation programs [2] most often rely on dc measurements [3] of the nonlinearity, e.g. the I/V curves. This can give suboptimum models because some transistor characteristics show a strong frequency dependence even in the linear operating range (e.g. the output conductance of GaAs MESFET's [4]). A recently published approach to microwave characterization of large-signal nonlinear operation uses a combination of load-pull measurements with the harmonic balance technique [5].

The measurement method presented in this paper tries to reach the same goal with a different approach: The series of harmonic frequencies generated in a nonlinear microwave device are measured directly. The vector measurement results can be interpreted as a nonlinear transfer function in the frequency domain. They may also be Fourier transformed to get a time-domain waveform. In this measurement system, the device is terminated with 50 Ω, not with the actual source and load impedances, as is done in the load-pull method [6]. The transfer function data alone do not characterize a device completely. Yet they are well suited to device characterization similar to what used to be done with time-domain waveform measurements [7]. The measurement data are also useful for the investigation of saturation mechanisms in devices analogous to [8], which is based on small-signal S parameters.

The presented measurement system has a better sensitivity than a sampling oscilloscope [9] due to its smaller noise bandwidth. In addition it does not suffer from the trigger jitter problems that often exist in microwave sampling oscilloscopes. In contrast to large-signal S-parameter measurements [10], [11], not only the fundamental but also the harmonics are measured. Frequency-domain errors of the measurement setup (e.g. dispersion) can be corrected easily, whereas in a time-domain measurement system an additional transformation is required [12].

Section II of the paper presents the concept of the measurement system. The phase calibration at the harmonic frequencies is discussed in Section III. Section IV summarizes the main factors that limit measurement accuracy. Finally, in Section V measurements of the first four harmonics (fundamental frequency $f_1 = 5$ GHz) of the MESFET NE 710 are compared with (i) direct power measurements with a scalar network analyzer, and (ii) time-domain waveforms measured with a sampling oscilloscope.

II. The Measurement Procedure

A. The Measurement System

The measurement system (Fig. 1) is built around a phase-locked signal generator with internal multiplication (Hewlett–Packard HP8350 with HP83595A RF plug-in) and an automatic vector network analyzer (ANA, type HP8410). In addition to the main output (0.01 to 26.5 GHz), the HP 83595A RF plug-in has an auxiliary output where the fundamental signal (2.3 to 7 GHz) is available. This signal (used here within the range 3.5 GHz $< f_1 <$ 6.5 GHz) is amplified and filtered to remove the harmonics. The input power P_{in} to the device under test (DUT) can be adjusted with the variable attenuator to a maximum of 13 dBm.

The bias T at the output of the DUT is followed by a 10 dB attenuator defining the load impedance for the DUT.

Manuscript received April 13, 1988; revised April 10, 1989.

The author is with the Institut für Feldtheorie und Höchstfrequenztechnik, Swiss Federal Institute of Technology (ETH) Zürich, CH-8092 Zürich, Switzerland.

IEEE Log Number 8929895.

0018-9480/89/1000-1506$01.00 ©1989 IEEE

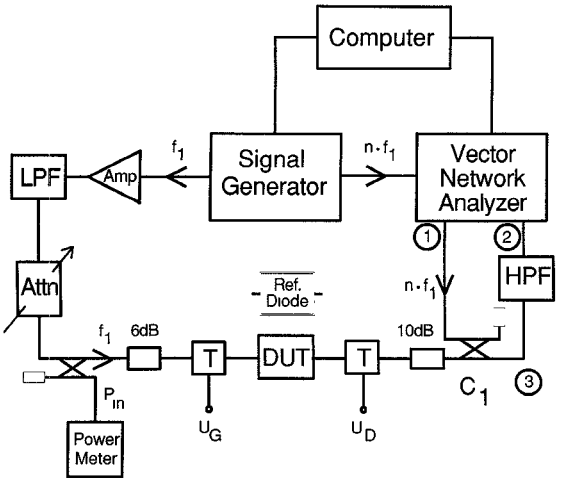

Fig. 1. Block diagram of the measurement system. f_1: fundamental frequency; $n \cdot f_1$: harmonic frequency where ANA is working; C_1: directional coupler (10 dB); T: bias tee; U_G: gate bias voltage (for a MESFET as DUT); U_D: drain bias voltage (MESFET); P_{in}: monitored input power.

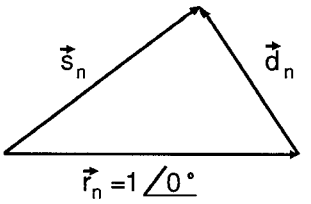

Fig. 2. The signal vectors at point 3 of the measurement system (components at the frequency $n \cdot f_1$).

The coupler C_1 adds the "reference signal" from port 1 of the ANA to the signal coming from the DUT. The directivity of this coupler is essential to prevent the reference signal from reaching the output of the DUT.

A high-pass filter (HPF) reduces the amplitude of the fundamental component to avoid an overload of port 2 of the ANA. Because of the inherent selectivity of the ANA harmonic converter, there is no need to eliminate the fundamental frequency (or the other harmonics) completely.

B. Harmonic Vector Measurement Procedure

The ANA operates at the frequency of the harmonic to be measured, fed by the multiplied output of the signal generator. It is configured for a forward transmission measurement from port 1 to port 2. During the standard forward response calibration of the network analyzer, the DUT is replaced by two matched loads. After this calibration, a forward transmission measurement of the signal coming from port 1 of the ANA has the results $1.0\angle 0°$. This is the reference signal vector $\vec{r}_n$ in Fig. 2.

The nonlinear device produces the component $\vec{d}_n$ at the frequency $n \cdot f_1$. The ANA measurement with the DUT in place gives the sum vector $\vec{s}_n$. Therefore, we can calculate the vector $\vec{d}_n$ from

$$\vec{d}_n = \vec{s}_n - \vec{r}_n = \vec{s}_n - 1.0. \tag{1}$$

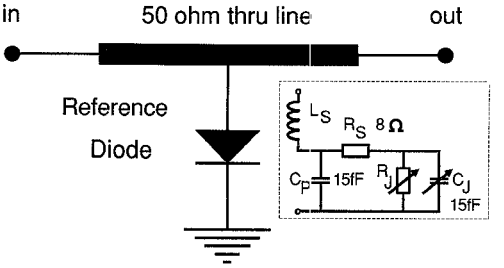

Fig. 3. The diode circuit for generating the reference harmonics with the diode equivalent circuit shown in the insert.

This is only the first step of the measurement procedure, because the raw measurement vectors $\vec{d}_n$ still are relative values (referred to the $\vec{r}_n$ vectors). For the calculation of the absolute magnitude $|a_n|$ the length of $\vec{r}_n$ is needed as a *reference power*. This reference power $P_{\text{ref},n}$ is obtained from a power meter connected to point 3 in Fig. 1 (with the DUT disconnected).

The voltage (magnitude) $|a_n|$ of the nth harmonic component can now be calculated with the impedance of the measurement system $Z_0 = 50\ \Omega$ as follows:

$$|a_n| = \sqrt{2} \cdot \sqrt{Z_0 \cdot |d_n|^2 \cdot P_{\text{ref},n}}. \tag{2}$$

The factor $\sqrt{2}$ converts average power to peak voltage. Of course, the attenuation from the DUT output to point 3 (10 dB attenuator, bias T, and coupler) must be included in the magnitude calculation.

The phase relation between the fundamental signal f_1 driving the DUT and the signal $n \cdot f_1$ feeding the ANA is *a priori* undefined. (The phase difference between the two outputs of the signal generator as well as the length differences in the measurement system is unknown.)

III. Phase Calibration at the Nth Harmonic

A. The Phase Reference Circuit

The key idea is to use a device which has a much faster switching time than the typical DUT as a "reference device." In the reference circuit (Fig. 3), a GaAs beam lead diode (Marconi DC 1346) is connected in parallel to a 50 Ω microstrip line. This circuit works as a limiter, clipping the top of the sine wave and thereby generating a well-defined spectrum of harmonics.

This diode is one of the fastest commercially available. The element values of the diode equivalent circuit are given in the insert of Fig. 3. Fig. 4 shows a photograph of the reference circuit built on 0.254-mm-thick (10 mil) Duroid 5880, mounted in a fixture with K connectors.

It is essential to keep the parasitics (in particular L_s and C_p) in the circuit small. This is evident from the two SPICE simulations of the phase of the harmonics shown in Fig. 5. For a worst-case L_s of 0.05 nH, the phase lag is $-8.8°$ at the third and $-15.6°$ at the fourth harmonic of $f_1 = 5$ GHz. If the series inductance L_s is below 0.05 nH, the deviation of the phase from the ideal value is much smaller. For the moment, the phase lag due to the nonideal

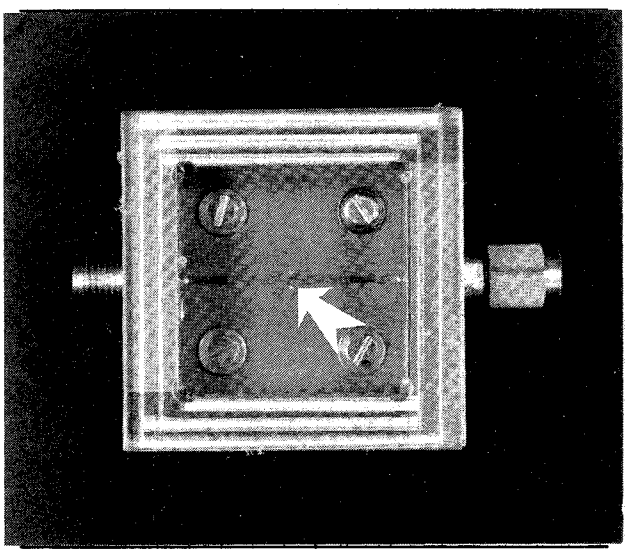

Fig. 4. Photograph of the diode circuit on 0.254 mm Duroid 5880 (circuit size: 25.4×25.4 mm², the white arrow points at the reference diode).

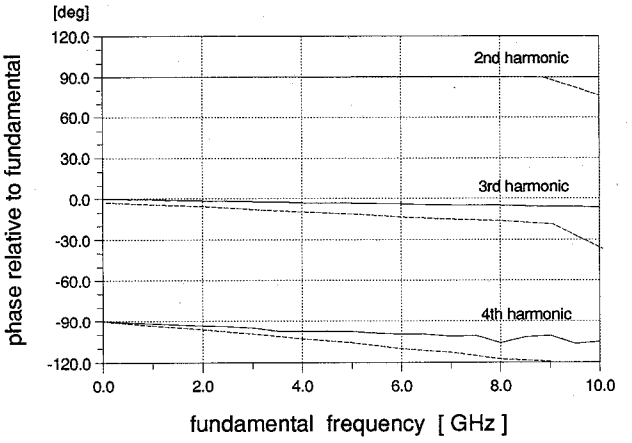

Fig. 5. SPICE simulation of reference diode phase of second, third, and fourth harmonics with $L_s = 0$ and $L_s = 0.05$ nH (solid lines: diode series inductance $L_s = 0$; dashed lines: diode series inductance $L_s = 0.05$ nH; phase relative to the fundamental described by $a_1(t) = |a_1| \cdot \sin(2\pi f_1 t + 0°)$, $P_{in} = 10$ dBm).

diode will be neglected. It is discussed further in Section IV.

With the circuit of Fig. 4 connected in place of the DUT, a *reference phase measurement* is taken with $P_{in} \approx 10$ dBm. The reference vector $\vec{d}_{r,n} = |d_{r,n}| \cdot e^{j\varphi_{r,n}}$ is then calculated for every harmonic n according to (1). Its angle is called the reference phase $\varphi_{r,n}$. Because the true phase relation at the reference diode is known, these reference phase values specify the actual phase relation in the measurement system. They can therefore be used for correction of the raw measurement vectors $\vec{d}_n$.

B. Calculation of the Corrected Phase

In the following, the fundamental and harmonic components are described by their complex amplitudes

$$a_n = |a_n| \cdot e^{j\alpha_n}, \qquad n = 1,2,3,\cdots. \tag{3}$$

(Note that this means that the fundamental is described by $a_1 = |a_1| \cdot \cos(2\pi f_1 t + \alpha_1)$.) Without loss of generality, the phase of the fundamental frequency term may be set to $\alpha_1 = 0°$ at one particular point in the system.

The measurement of the DUT at a specific input power level has given a set of raw measurement vectors $\vec{d}_n = |d_n| \cdot e^{j\varphi_n}$. The reference phase measurement has yielded a set of reference phase values $\varphi_{r,n}$.

From the Fourier series of the top-clipped sine wave produced in the reference circuit and using the notation in (3), the true phase of the nth harmonic, with reference to $\alpha_1 = 0°$ at the DUT input, is now given by

$$\alpha_n = \varphi_n - \varphi_{r,n} - 180° \qquad (2 \leqslant n \leqslant 4). \tag{4}$$

The correction term of $-180°$ is valid for an ideally limiting diode mounted with its cathode to ground (as shown in Fig. 3).

Any electrical length difference between the diode reference circuit and the DUT must be considered in the phase calculation. When microstrip or another dispersive line type is used in the DUT fixture, it is best to measure the transmission phase of the path from the DUT output connector to point 3 at all frequencies of interest $n \cdot f_1$.

The transfer function of the DUT at the fundamental frequency (i.e., the large-signal S_{21}) can also be determined with the setup of Fig. 1. In this case a through line without diode is used for phase calibration.

TABLE I
HARMONIC COMPONENTS AT THE DRAIN OF A NE 710-83 FOR THREE DIFFERENT BIAS CONDITIONS AT $f_1 = 5$ GHz (I_{D0}: BIAS CURRENT WITHOUT RF EXCITATION)

a) Bias conditions: U_D = 3 V, U_G = -1 V

P_{in}	f_0		2 f_0		3 f_0		4 f_0	
	mag.	phase	mag.	phase	mag.	phase	mag.	phase
[dBm]	[mV]	[deg.]	[mV]	[deg.]	[mV]	[deg.]	[mV]	[deg.]
2	316	84.7	151	22.5	26.8	-59.7	12.2	64.4
4	476	83.8	215	19.2	30.5	-71.8	23.8	57.4
6	714	85.9	307	19.9	31.6	-80.3	37.6	52.8
8	1010	84.5	414	15.8	33.5	-108.0	56.9	44.9
10	1414	85.1	566	15.6	39.4	-129.7	81.1	43.3

b) Bias conditions: U_D = 3 V, I_{Do} = 5 mA

P_{in}	f_0		2 f_0		3 f_0		4 f_0	
	mag.	phase	mag.	phase	mag.	phase	mag.	phase
[dBm]	[mV]	[deg.]	[mV]	[deg.]	[mV]	[deg.]	[mV]	[deg.]
2	775	83.0	170	5.0	33.2	-244.9	6.5	-27.5
4	975	82.3	235	3.9	42.9	-245.1	13.8	-1.5
6	1229	82.8	316	6.8	54.4	-229.6	24.0	8.5
8	1546	81.8	412	4.5	70.6	-236.6	39.5	7.9
10	1916	82.5	529	6.5	104.5	-239.6	74.7	9.7

c) Bias conditions: U_D = 3 V, U_G = 0 V ($I_D = I_{Dss}$)

P_{in}	f_0		2 f_0		3 f_0		4 f_0	
	mag.	phase	mag.	phase	mag.	phase	mag.	phase
[dBm]	[mV]	[deg.]	[mV]	[deg.]	[mV]	[deg.]	[mV]	[deg.]
2	1261	74.7	20.5	-32.2	2.8	-239.2	0.8	-54.4
4	1584	75.1	30.5	-32.6	7.7	-272.6	1.7	-22.6
6	1957	76.5	38.0	-24.8	32.1	-273.9	8.2	-42.4
8	2207	78.2	93.5	-9.9	114.5	-270.5	19.1	-80.0
10	2293	82.3	249.0	5.9	217.0	-254.9	58.4	-55.3

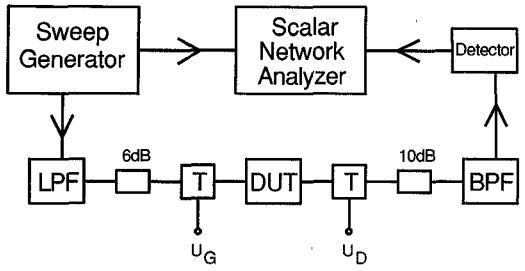

Fig. 6. The setup used for the direct power measurement of harmonics (same abbreviations as in Fig. 1).

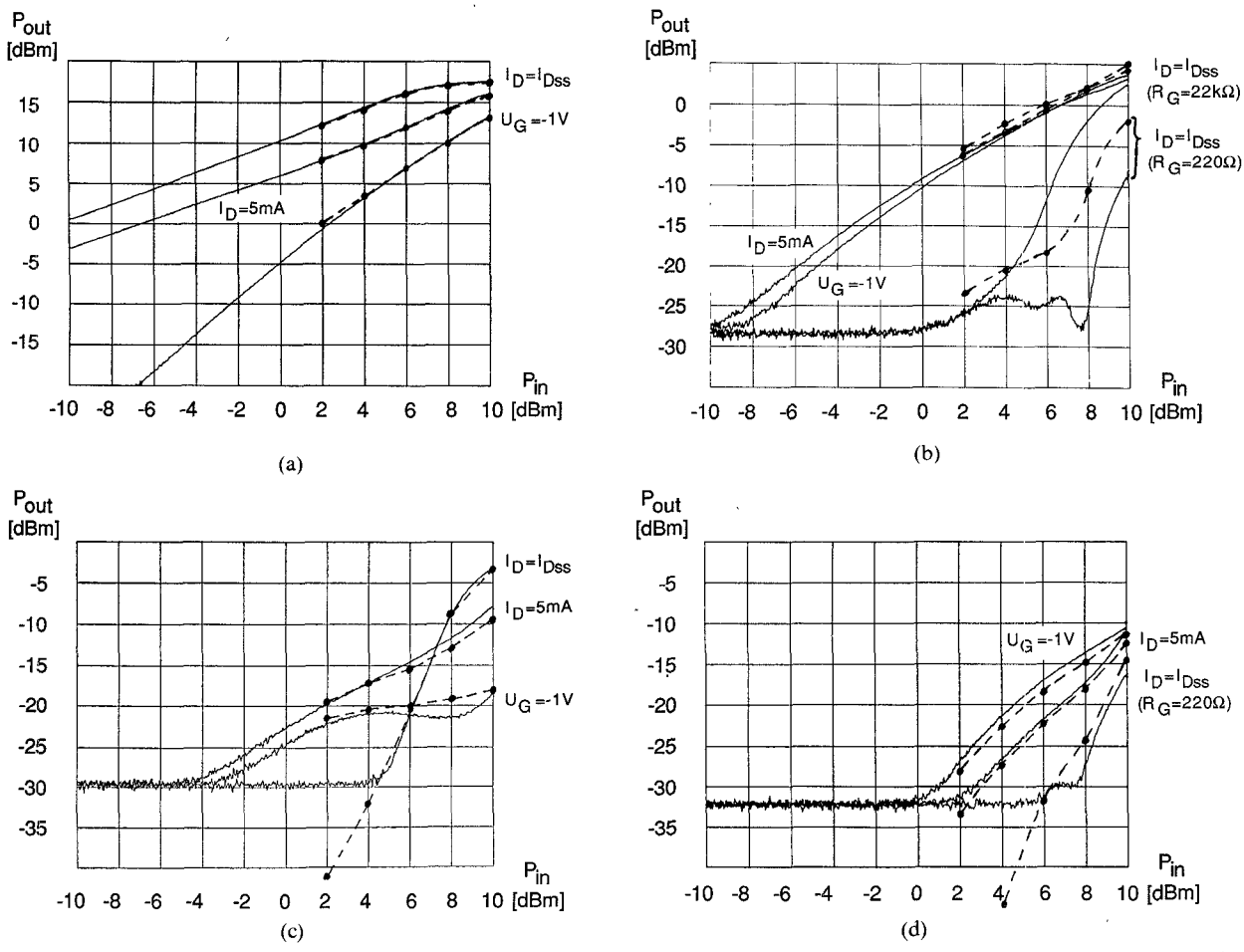

Fig. 7. The magnitude of the first four harmonics of an NEC NE 710-83 biased at $U_D = 3$ V measured by the described system (broken lines) and compared with direct power measurements (solid lines). (a) Fundamental at 5 GHz. (b) Second harmonic at 10 GHz. (c) Third harmonic at 15 GHz. (d) Fourth harmonic at 20 GHz.

IV. Measurement Errors and How to Avoid Them

A brief discussion of the main errors in the measurement procedure concentrates on the following four points:

1) Reference Device Error: With the present reference circuit the phase error due to the reference device is below 10° at 15 GHz and less than 16° at 20 GHz for $f_1 =$ 5 GHz. In all the simulation runs, the real device (with parasitics) had a phase lag compared to an ideal one. At present, this phase lag is not accounted for because of the uncertainty remaining in the characterization of the diode equivalent circuit. (The diode capacitances C_j and C_p and the inductance L_s are too small to be measured with the required accuracy.)

Another difficulty with the reference circuit is the dependence of the reference phase on the incident power. On the one hand, the power level during the reference measurement should be low to avoid exciting the nonlinear capacitances of the diode too much. On the other hand, the level must be high enough to let the desired harmonic

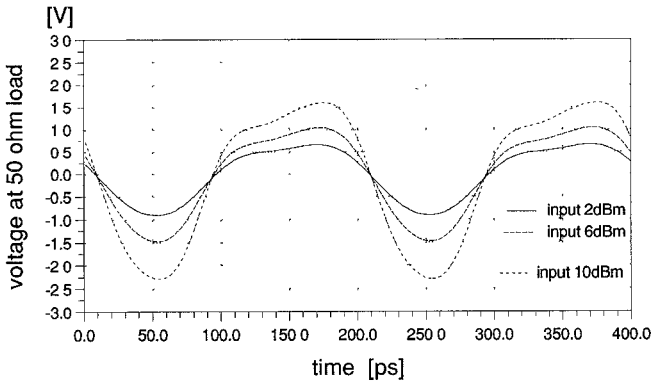

Fig. 8. The time-domain waveform of the drain voltage (sum of the first four harmonics of $f_1 = 5$ GHz, measured at $U_D = 3$ V, $I_{D0} = 5$ mA).

stand out of the noise. A power of 10 dBm is a good compromise.

2) Accuracy of the Network Analyzer: For low-level harmonics, accuracy is limited by ANA magnitude and phase uncertainty. (Note that the sum vector $\vec{s}$ can reach the noise floor of the ANA only if the harmonic signal out of the DUT exactly cancels the reference signal from the ANA.) For high-level harmonics, compression in the ANA limits the accuracy.

3) Power Measurement Error: In addition to the power meter uncertainty, subharmonics and spurious signals of the signal generator may reduce the accuracy of the reference power measurement. A filter inserted between port 1 of the ANA and the coupler C_1 can reduce spurious and broad-band noise.

4) Mismatch in the Measurement Setup: If it is not negligible ($|r| \ll 0.1$), it must at least be kept as constant as possible. This applies to ANA calibration, harmonic phase calibration, and DUT measurement.

V. Measurement Results

The harmonics generated in the small-signal MESFET NEC NE 710-83 have been measured with the described method. The reference diode was considered ideal. Data on the first four harmonics of $f_1 = 5$ GHz for three different bias conditions and five input power levels are listed in Table I.

To check the performance of the measurement system (in particular the procedure described by (1) and (2)), the magnitude values have been compared with results from the power measurement system shown in Fig. 6.

Fig. 7 shows plots of the direct power measurements (solid lines) and the points measured with the presented system (connected by broken lines). The coincidence of the curves in general is good. The only exception is the second harmonic (Fig. 7(b)) at $I_D = I_{Dss}$, which shows a particularly strong dependence on the dc series resistance in the gate circuit. Fig. 7(c) and (d) clearly show the advantage of the new method for measuring harmonics with small amplitudes which are buried in the broad-band noise of the power measurement system. (The broad-band noise floor in Fig. 7 is 15 $\cdots$ 20 dB higher than the tangential sensitivity of the detector because of the attenuator and the insertion loss of the filter.)

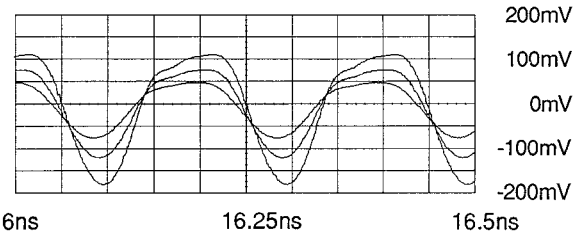

Fig. 9. Plot of a direct waveform measurement with the HP54120T digital sampling oscilloscope (same input power and bias as in Fig. 8, but without correction of cable loss).

To check the validity of the phase measurement, the series of (complex) harmonic frequencies can be transformed to the time domain. Fig. 8 shows the drain voltage waveform of the NE 710 biased at $U_D = 3$ V with a quiescent current I_{D0} of 5 mA. (The dc component is omitted in this figure.)

The output waveforms are plotted for three different input power levels (2, 6, and 10 dBm). For comparison, Fig. 9 shows the output waveform of the same device (with the same bias setting) measured on a HP 54120T digitizing sampling oscilloscope. The amplitude in Fig. 9 must be corrected for a loss of 20 dB in the power splitter feeding the trigger input and an additional 1–2 dB of frequency-dependent cable loss. Taking this into account, the coincidence of the two sets of curves is good.

VI. Conclusions

The described system allows the measurement of harmonics with a phase accuracy of about $\pm 10°$ at 20 GHz (referred to $f_1 = 5$ GHz). It can be built for any frequency (< 40 GHz) where a vector network analyzer and a suitable signal generator with multiplier are available. For low-amplitude harmonics, the higher sensitivity compared to time-domain measurements with a sampling scope results in better measurement accuracy. The accuracy should improve further if the nonideality of the diode reference circuit can be characterized more precisely. Measurements with a non-50-Ω load could be performed by the addition of fundamental frequency load-pull similar to the method described in [13].

Acknowledgment

The author would like to thank R. Hügli for the many technical discussions and H. R. Benedickter for help in solving network analyzer problems.

References

[1] H. Kondoh, "An accurate FET modelling from measured *S*-parameters," *1986 IEEE MTT-S Int. Microwave Symp. Dig.*, pp. 377–380.

[2] H. Statz *et al.*, "GaAs FET device model and circuit simulation in SPICE," *IEEE Trans. Electron Devices*, vol ED-34, pp 160–169, Feb. 1987.

[3] H. Fukui, "Determination of the basic device parameters of a GaAs MESFET," *Bell Syst. Tech. J.*, vol. 58, pp. 771–797, Mar. 1979.

[4] C. Camacho-Penalosa and C. S. Aitchison, "Modelling frequency dependence of output impedance of a microwave MESFET at low

frequencies," *Electron. Lett.*, vol. 21, no. 12, pp. 528–529, 6 June 1985.
[5] B. R. Epstein *et al.*, "Large-signal MESFET characterization using harmonic balance," in *1988 IEEE MTT-S Int. Microwave Symp. Dig.*, pp. 1045–1048.
[6] D. Poulin, "Load-pull measurements help you meet your match," *Microwaves*, pp. 61–65, Nov. 1980.
[7] F. Sechi, H. Huang, and B. Perlman, "Waveform and saturation in GaAs power MESFETs," in *Proc. 8th European Microwave Conf.*, 1978, pp. 473–477.
[8] M. R. Weiss and D. Pavlidis, "An investigation of the power characteristics and saturation mechanisms in HEMT's and MESFET's," *IEEE Trans. Electron Devices*, vol. 35, pp. 1197–1206, Aug. 1988.
[9] W. M. Gove, "Sampling for oscilloscopes and other RF systems: DC through *X*-band," *IEEE Trans. Microwave Theory Tech.*, vol. MTT-14, pp. 629–638, Dec. 1966.
[10] W. H. Leighton, R. J. Chaffin, and J. G. Webb, "RF amplifier design with large-signal *S*-parameters," *IEEE Trans. Microwave Theory Tech.*, vol. MTT-21, pp. 809–814, Dec. 1973.
[11] S. R. Mazumder and P. D. van der Puije, "'Two-signal' method of measuring the large signal *S*-parameters of transistors," *IEEE Trans. Microwave Theory Tech.*, vol. MTT-26, pp. 417–420, June 1978.
[12] M. Sipilä, K. Lehtinen, and V. Porra, "High frequency periodic time-domain waveform measurement system," *IEEE Trans. Microwave Theory Tech.*, vol. 36, pp. 1397–1405, Oct. 1988.
[13] Y. Takayama, "A new load-pull characterization method for microwave power transistors," in *1976 IEEE MTT-S Int. Microwave Symposium Dig.*, pp. 218–220.

✠

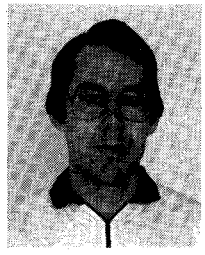

Urs Lott (S'81) was born in Zürich, Switzerland, in 1959. He received the Dipl. Ing. degree in electrical engineering from the Swiss Federal Institute of Technology, Zürich, in 1983. He is presently employed as a Research Assistant in the Group for Microwave Electronics at the same university, working towards the Ph.D. degree. His main interests are the measurement and modeling of GaAs FET's and the application of active devices to nonlinear microwave circuits.